cussed in T. Borén and P. Falk, *Sci. Am. Sci. Med.* **1**, 28 (April 1994); L. S. Tompkins and S. Falkow, *Science* **267**, 1621 (1995).
29. M. J. Blaser, *Lancet* **349**, 1020 (1997).
30. H. Clausen and S. Hakomi, *Vox Sang.*, **56**, 1 (1989).
31. We thank Q. Jiang and D. E. Taylor for analysis of the locations of the *babA* and *babB* genes; R. Gilman for *H. pylori* strain P119; K. A. Eaton for *H. pylori* strain 26695; P.-I. Ohlsson for NH_2-terminal sequencing; J. Van Beeumen and B. Samyn for COOH-terminal sequencing; R. Rosqvist for assistance with confocal microscopy; L. Johansson for assistance with electron microscopy; M. Block for image processing; R. Rappual for suggestions; Z. Xiang and S. Guidotti for strains; and D. L. Milton, J. Carlsson, B.-E. Uhlin, and P. Falk for critical reading of the manuscript. Supported by the Swedish Society of Medicine, Lion's Cancer Research Foundation, Umeå University, the Magnus Bergvall Foundation (T.B.), the Swedish Medical Research Council [grants 11218 (T.B.), 10848 (L.E.), and 7480 (L. Björck)], the Swedish Society for Medical Research (T.B. and D.I.), the Royal Swedish Academy of Sciences, the J. C. Kempe Memorial Foundation (D.I.), the Umeå University–Washington University Scientific Exchange Program (T.B. and J.Ö.), and grants from the NIH and American Cancer Society (D.E.B.) and from Chiron Co. (A.C.).

19 September 1997; accepted 2 December 1997

Cancer Treatment by Targeted Drug Delivery to Tumor Vasculature in a Mouse Model

Wadih Arap,* Renata Pasqualini,* Erkki Ruoslahti†

In vivo selection of phage display libraries was used to isolate peptides that home specifically to tumor blood vessels. When coupled to the anticancer drug doxorubicin, two of these peptides—one containing an α_v integrin–binding Arg-Gly-Asp motif and the other an Asn-Gly-Arg motif—enhanced the efficacy of the drug against human breast cancer xenografts in nude mice and also reduced its toxicity. These results indicate that it may be possible to develop targeted chemotherapy strategies that are based on selective expression of receptors in tumor vasculature.

Endothelial cells in the angiogenic vessels within solid tumors express several proteins that are absent or barely detectable in established blood vessels (*1*), including α_v integrins (*2*) and receptors for certain angiogenic growth factors (*3*). We have applied in vivo selection of phage peptide libraries to identify peptides that home selectively to the vasculature of specific organs (*4*, *5*). The results of our studies imply that many tissues have vascular "addresses." To determine whether in vivo selection could be used to target tumor blood vessels, we injected phage peptide libraries into the circulation of nude mice bearing human breast carcinoma xenografts.

Recovery of phage from the tumors led to the identification of three main peptide motifs that targeted the phage into the tumors (*6*). One motif contained the sequence Arg-Gly-Asp (RGD) (*7*, *8*), embedded in a peptide structure that we have shown to bind selectively to $\alpha_v\beta_3$ and $\alpha_v\beta_5$ integrins (*9*). Phage carrying this motif, CDCRGDCFC (termed RGD-4C), homes to several tumor types (including carcinoma, sarcoma, and melanoma) in a highly selective manner, and homing is specifically inhibited by the cognate peptide (*10*).

A second peptide motif that accumulated in tumors was derived from a library with the general structure $CX_3CX_3CX_3C$ (X = variable residue, C = cysteine) (*6*). This peptide, CNGRCVSGCAGRC, contained the sequence Asn-Gly-Arg (NGR), which has been identified as a cell adhesion motif (*11*). We tested two other peptides that contain the NGR motif but are otherwise different from CNGRCVSGCAGRC: a linear peptide, NGRAHA (*11*), and a cyclic peptide, CVLNGRMEC. Tumor homing for all three peptides was independent of the tumor type and species; the phage homed to a human breast carcinoma (Fig. 1A), a human Kaposi's sarcoma, and a mouse melanoma (*12*). We synthesized the minimal cyclic NGR peptide from the CNGRCVSGCAGRC phage and found that this peptide (CNGRC), when coinjected with the phage, inhibited the accumulation of the CNGRCVSGCAGRC phage (Fig. 1A) and of the two other NGR-displaying phages in breast carcinoma xenografts (*12*).

The third motif—Gly-Ser-Leu (GSL) and its permutations—was frequently recovered from screenings using breast carcinoma (*6*), Kaposi's sarcoma, and malignant melanoma, and homing of the phage was inhibited by the cognate peptide (Fig. 1B). This motif was not studied further here.

The RGD-4C phage homes selectively to breast cancer xenografts (Fig. 1C). This homing can be inhibited by the free RGD-4C peptide (*10*), but not by the CNGRC peptide, even when this peptide was used in amounts 10 times those that inhibited the homing of the NGR phage (Fig. 1D). Tumor homing of the NGR phage was also partially inhibited by the RGD-4C peptide (Fig. 1E), but this peptide was only 10 to 20% as potent as CNGRC. An unrelated cyclic peptide, GACVFSIAHECGA, had no effect on the tumor-homing ability of either phage (*12*). Thus, our in vivo screenings yielded two peptide motifs, RGD-4C and NGR, both of which had previously been reported

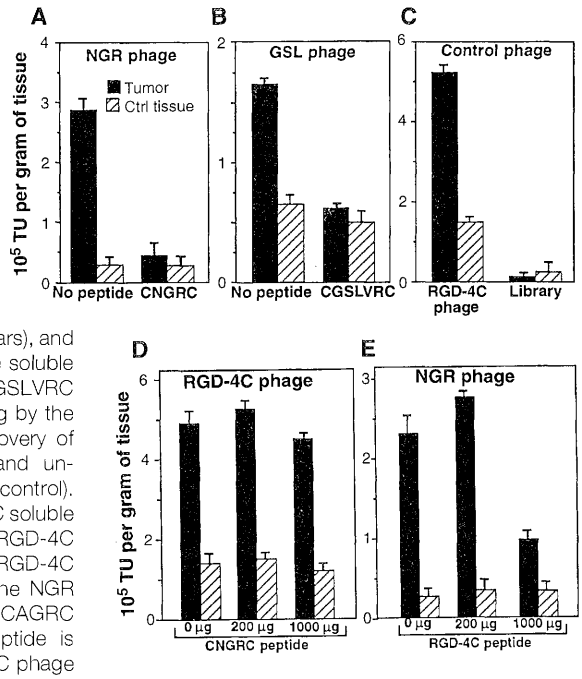

Fig. 1. Recovery of phage displaying tumor-homing peptides from breast carcinoma xenografts. Phage [10^9 transducing units (TU)] was injected into the tail vein of mice bearing size-matched MDA-MB-435–derived tumors (~1 cm^3) and recovered after perfusion. Mean values for phage recovered from the tumor or control tissue (brain) and the SEM from triplicate platings are shown. (**A**) Recovery of CNGRCVSGCAGRC phage from tumor (solid bars) and brain (striped bars), and inhibition of the tumor homing by the soluble peptide CNGRC. (**B**) Recovery of CGSLVRC phage and inhibition of tumor homing by the soluble peptide CGSLVRC. (**C**) Recovery of RGD-4C phage (positive control) and unselected phage library mix (negative control). (**D**) Increasing amounts of the CNGRC soluble peptide were injected with the RGD-4C phage. (**E**) Increasing amounts of the RGD-4C soluble peptide were injected with the NGR phage. Inhibition of the CNGRCVSGCAGRC phage homing by the CNGRC peptide is shown in (A); inhibition of the RGD-4C phage by the RGD-4C peptide has been reported (*10*).

Cancer Research Center, The Burnham Institute, 10901 North Torrey Pines Road, La Jolla, CA 92037, USA.

*These authors contributed equally to this report.
†To whom correspondence should be addressed. E-mail: ruoslahti@burnham-inst.org

to bind to integrins (*9*, *11*). The affinity of NGR for integrins is about three orders of magnitude less than that of RGD peptides (*7*, *11*). Nevertheless, the homing ratio (tumor/control organ) of the phage displaying the NGR motif was three times that of the RGD-4C phage (*12*). This discrepancy in activities, and the cross-inhibition results described above, strongly suggest that the NGR and RGD-4C peptides bind to different receptors in the tumors.

We next studied phage homing to tumors by immunostaining (Fig. 2). In one set of experiments (*13*), phage was allowed to circulate for 3 to 5 min, followed by perfusion (*10*) and immediate tissue recovery. In the second set, tissues were analyzed 24 hours after phage injection, when there is almost no phage left in the circulation (*10*). Strong phage staining in tumor vasculature, but not in normal endothelia, was seen in the short-term experiments with CNGRCVSGCAGRC phage in MDA-MB-435 cell–derived human breast carcinoma xenografts (Fig. 2A) and SLK cell–derived human Kaposi's sarcoma xenografts (Fig. 2B). The two other NGR phages, NGRAHA and CVLNGRMEC, also showed strong tumor staining (*12*), whereas a control phage showed no staining (Fig. 2, E and F). At 24 hours, the staining pattern indicated that the NGR phage had spread outside the blood vessels and into the tumors (Fig. 2, C and D). This spreading may be attributable to increased permeability of tumor blood vessels (*14*) or uptake of the phage by angiogenic endothelial cells (*15*) and subsequent transfer to tumor tissue.

The CNGRCVSGCAGRC phage showed the greatest tumor selectivity among all the peptides analyzed. Several control organs showed very low or no immunostaining, confirming the specificity of the NGR motif for tumor vessels; heart (Fig. 2G) and mammary gland (Fig. 2H) are shown (*16*). Spleen and liver, which are part of the reticuloendothelial system (RES), contained phage; uptake by the RES is a general property of the phage particle and is independent of the peptide it displays (*10*, *17*). These immunostaining results with the NGR phage are similar to observations made with the RGD-4C phage (*10*).

To determine whether the tumor-homing peptides RGD-4C and CNGRC could be used to improve the therapeutic index of cancer chemotherapeutics, we coupled them to doxorubicin (dox) (*18*). Dox is one of the most frequently used anticancer drugs and one of a few chemotherapeutic agents known to have antiangiogenic activity (*19*). The dox-peptide conjugates were used to treat mice bearing tumors derived from human MDA-MB-435 breast carcinoma cells.

The commonly used dose of dox in nude mice with human tumor xenografts is 50 to 200 μg/week (*20*). Because we expected the dox conjugates to be more effective than the free drug, we initially used the conjugates at a dose of dox-equivalent of only 5 μg/week (*13*, *21*). Tumor-bearing mice treated with RGD-4C conjugate outlived the control mice, all of which died from widespread disease (Log-Rank test, $P < 0.0001$; Wilcoxon test, $P = 0.0007$) (Fig. 3A). In a dose-escalation experiment, tumor-bearing mice were treated with the dox-RGD-4C conjugate at 30 μg of dox-equivalent every 21 days for 84 days and were then observed, without further treatment, for an extended period of time. All of these mice outlived the dox-treated mice by more than 6 months, suggesting that both primary tumor growth and metastasis were inhibited by the conjugate. Many of the tumors in the mice that received the dox-RGD-4C conjugate (30 μg of dox-equivalent every 21 days) showed marked skin ulcer-

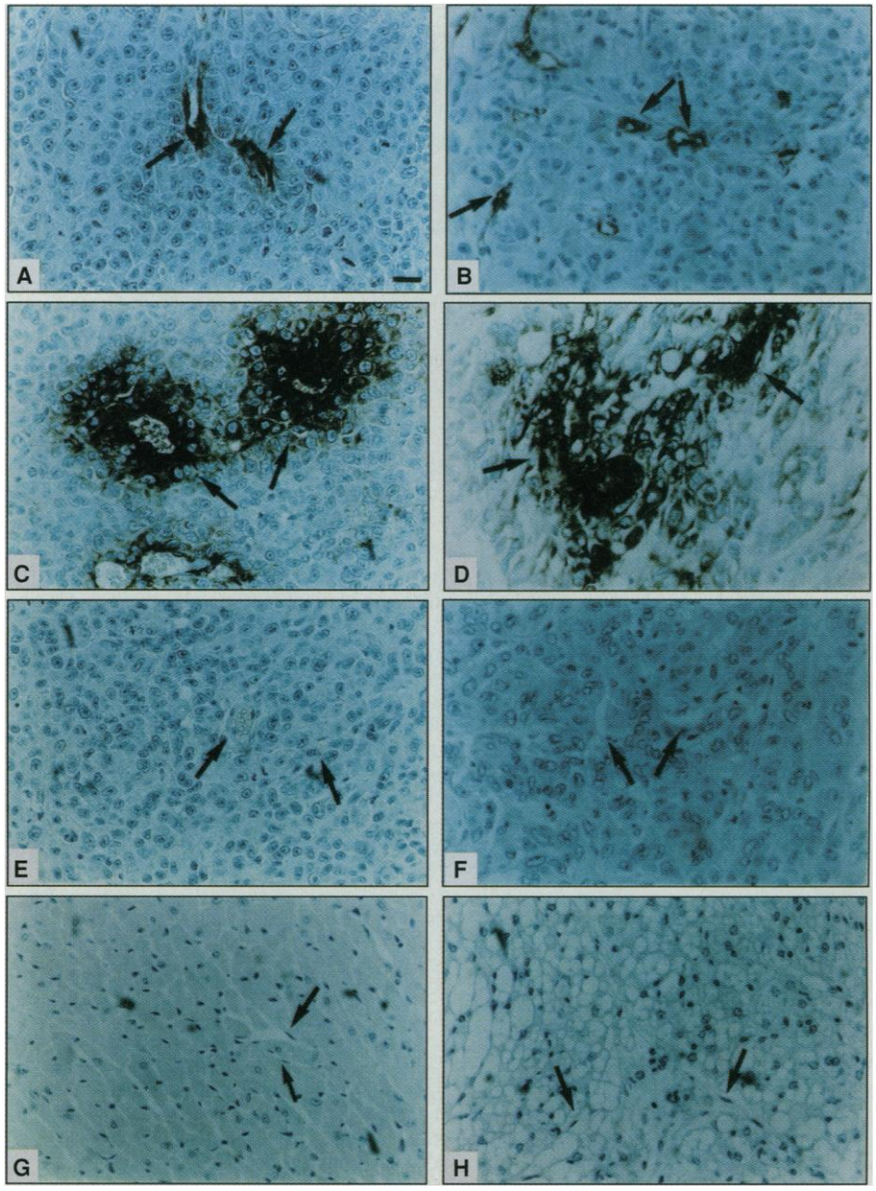

Fig. 2. Immunohistochemical staining of phage after intravenous injection into tumor-bearing mice. Phage displaying the peptide CNGRCVSGCAGRC (**A** to **D**, **G**, and **H**) or control phage with no insert (**E** and **F**) were injected intravenously into mice bearing MDA-MB-435–derived breast carcinoma (A, C, and E) and SLK-derived Kaposi's sarcoma (B, D, and F) xenografts. Phage was allowed to circulate for 4 min (A, B, E, and F) or for 24 hours (C, D, G, and H). Tumors and control organs were removed, fixed in Bouin solution, and embedded in paraffin for preparation of tissue sections. An antibody to M-13 phage (Pharmacia) was used for the staining. Heart (G) and mammary gland (H) are shown as control organs (*16*). Arrows point to blood vessels. Scale bar in (A), 5 μm.

ation and tumor necrosis, whereas these signs were not observed in any of the control groups. At necropsy, the mice treated with the dox-RGD-4C conjugate had significantly smaller tumors (t test, $P = 0.02$), less spreading to regional lymph nodes ($P < 0.0001$), and fewer pulmonary metastases ($P < 0.0001$) than did the mice treated with free dox (Fig. 3, B to D). Similar results were obtained in five independent experiments. Histopathological analysis revealed pronounced destruction of the tumor architecture and widespread cell death in the tumors of mice treated with the dox-RGD-4C conjugate; tumors treated with free dox at this dose were only minimally affected. In contrast, the dox-RGD-4C conjugate was less toxic to the liver and heart than was free dox (Fig. 3E). In some experiments, dox together with unconjugated soluble peptide was used as a control; the drug-peptide combination was no more effective than free dox (*12*).

To assess toxicity, we used 200 μg of dox-equivalent in mice with large (~5 cm^3), size-matched tumors (*13*, *21*). Mice treated with the dox-RGD-4C conjugate survived more than a week, whereas all of the dox-treated mice died within 48 hours of drug administration (Fig. 3F). Accumulation of dox-RGD-4C within the large tumors thus appeared to have sequestered the conjugated drug, thereby reducing its toxicity to other tissues.

Less extensive data with the CNGRC peptide conjugate indicated an efficacy similar to that of the RGD-4C conjugate. In all experiments, tumors treated with the dox-CNGRC conjugate were one-fourth to one-fifth as large as tumors treated in the control groups (Fig. 4A). A marked reduction in metastasis and a prolongation of long-term survival were also seen (Log-Rank test, $P = 0.0064$; Wilcoxon test, $P = 0.0343$) (Fig. 4B). Two of the six dox-CNGRC–treated animals were still alive more than 11 weeks after the last of the control mice died. The dox-CNGRC conjugate was also less toxic than the free drug (Fig. 4C). CNGRC peptide alone failed to reproduce the effect of the conjugate, even in doses up to 150 μg/week. Unconjugated CNGRC-dox mixture

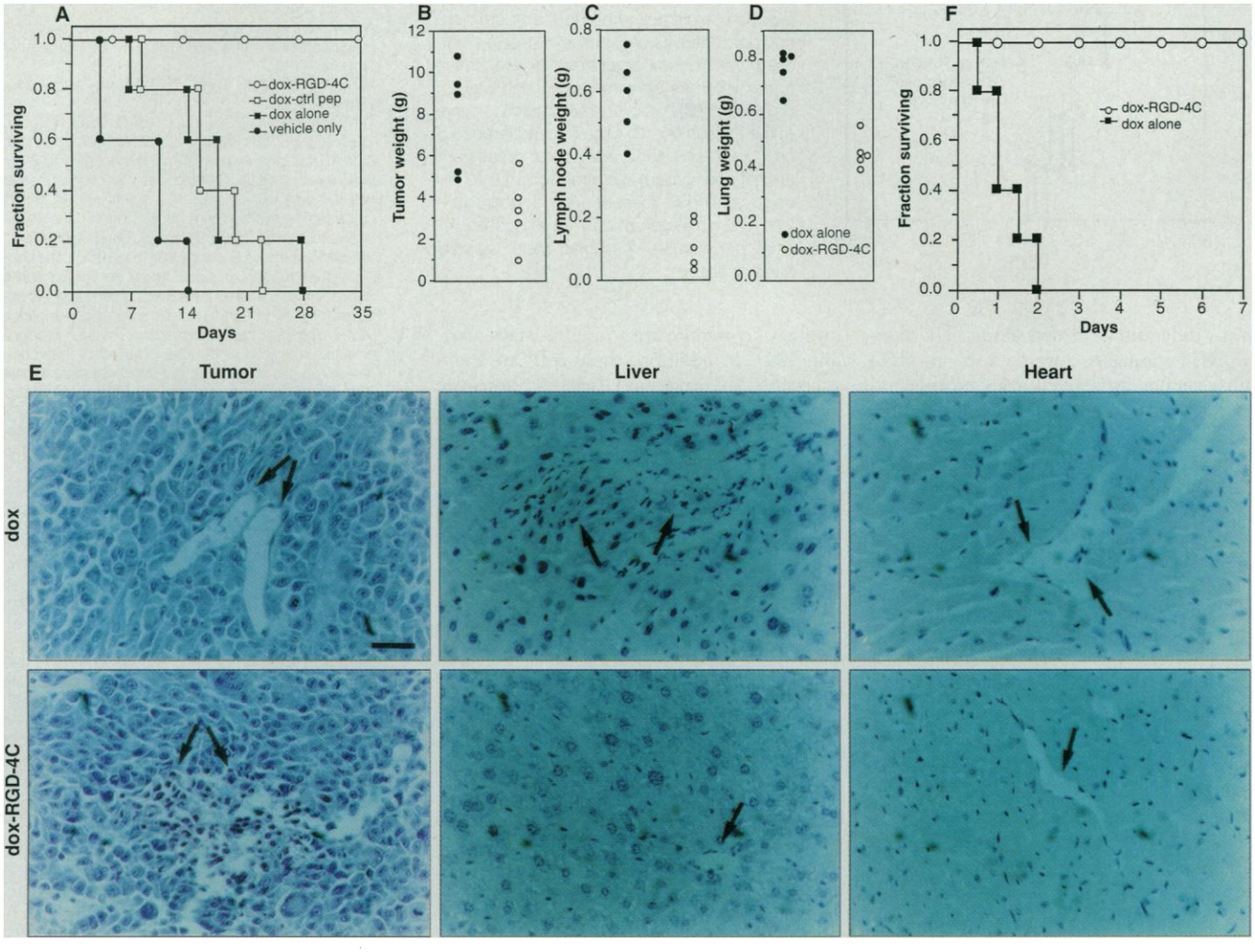

Fig. 3. Treatment of mice bearing MDA-MB-435–derived breast carcinomas with dox-RGD-4C peptide conjugate. Mice with size-matched tumors (~1 cm^3) were randomized into four treatment groups (five animals per group): vehicle only, free dox, dox-control peptide (GACVFSIAHECGA; dox-ctrl pep), and dox-RGD-4C conjugate. (**A**) Mice were treated with 5 μg/week of dox-equivalent. A Kaplan-Meier survival curve is shown. (**B** to **D**) Mice were treated with 30 μg of dox-equivalent every 21 days. The animals were killed, and tumors (B), axillary lymph nodes (C), and lungs (D) were weighed after three treatments. (**E**) Histopathological analysis (hematoxylin and eosin stain) of MDA-MB-435 tumors, liver, and heart treated with dox or dox-RGD-4C conjugate. Vascular damage was observed in the tumors treated with dox-RGD-4C conjugate (arrows, lower left panel), but not in the tumors treated with free dox (arrows, upper left panel). Signs of toxicity were seen in the liver and heart of mice treated with dox (arrows, upper middle and upper right panels), whereas the blood vessels were relatively undamaged in the mice treated with the dox-RGD-4C conjugate. The changes were scored blindly by a pathologist; representative micrographs are shown. Scale bar, 7.5 μm. (**F**) Mice bearing large (~5 cm^3) MDA-MB-435 breast carcinomas (four animals per group) were randomized to receive a single dose of free dox or dox-RGD-4C conjugate at 200 μg of dox-equivalent per mouse. A Kaplan-Meier survival curve is shown.

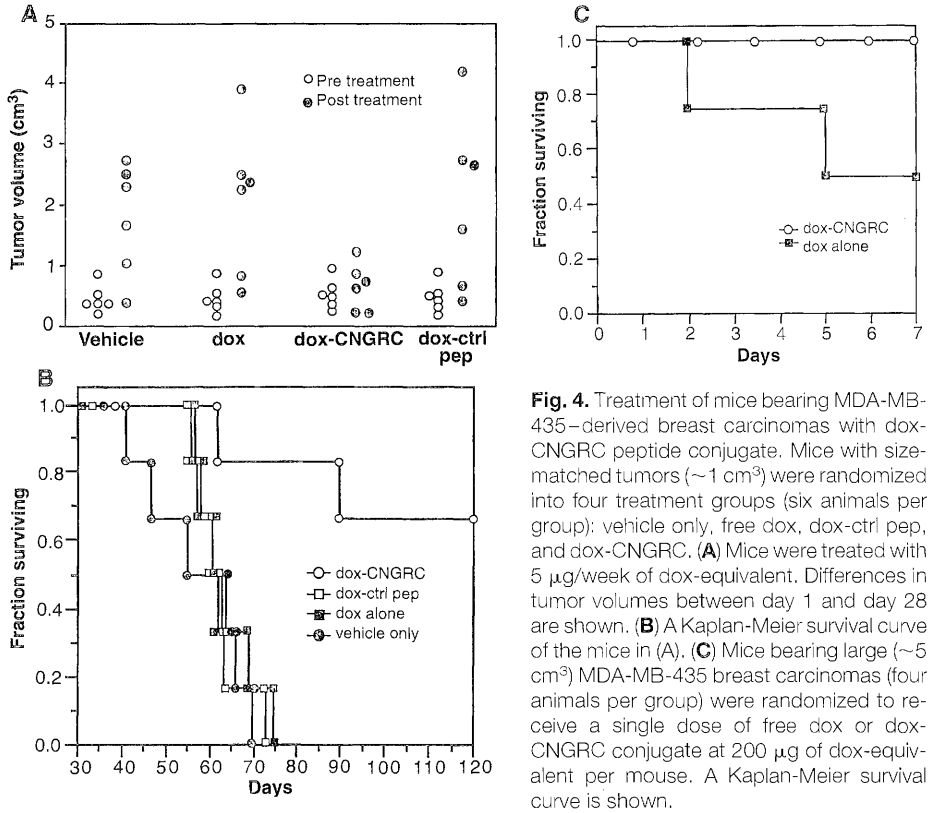

Fig. 4. Treatment of mice bearing MDA-MB-435–derived breast carcinomas with dox-CNGRC peptide conjugate. Mice with size-matched tumors (~1 cm^3) were randomized into four treatment groups (six animals per group): vehicle only, free dox, dox-ctrl pep, and dox-CNGRC. (**A**) Mice were treated with 5 μg/week of dox-equivalent. Differences in tumor volumes between day 1 and day 28 are shown. (**B**) A Kaplan-Meier survival curve of the mice in (A). (**C**) Mice bearing large (~5 cm^3) MDA-MB-435 breast carcinomas (four animals per group) were randomized to receive a single dose of free dox or dox-CNGRC conjugate at 200 μg of dox-equivalent per mouse. A Kaplan-Meier survival curve is shown.

was no different from dox alone. The dox-CNGRC conjugates were also effective against xenografts derived from another human breast carcinoma cell line, MDA-MB-231 (*12*).

We expect the NGR and RGD-4C motifs to target human vasculature as well, because (i) the NGR phage binds to blood vessels of human tumors and less so than to vessels in normal tissue (*22*), and (ii) the RGD-4C peptide binds to human α_v integrins (*9*, *10*), which are known to be selectively expressed in human tumor blood vessels (*23*). Thus, these peptides are potentially suitable for tumor targeting in patients. The RGD-4C peptide is likely to carry dox into the tumor vasculature and also to the tumor cells themselves, because the MDA-MB-435 breast carcinoma expresses α_v integrins (*10*). Because many human tumors express the α_v integrins (*23*), our animal model is a reasonable mimic of the situation in at least a subgroup of cancer patients. The targeting of drugs into tumors is a new use of the selective expression of α_v integrins and other receptors in tumor vasculature. The effectiveness of the CNGRC conjugate may be derived entirely from vascular targeting because the NGR peptides do not bind to the MDA-MD-435 cells (*12*).

The tumor vasculature is a particularly suitable target for cancer therapy because it is composed of nonmalignant endothelial cells that are genetically stable and therefore unlikely to mutate into drug-resistant variants (*24*). In addition, these cells are more accessible to drugs and have an intrinsic amplification mechanism; it has been estimated that elimination of a single endothelial cell can inhibit the growth of 100 tumor cells (*24*). New targeting strategies, including the ones described here, have the potential to markedly improve cancer treatment.

REFERENCES AND NOTES

1. J. Folkman, *Nature Med.* **1**, 27 (1995); W. Risau and I. Flamme, *Annu. Rev. Cell Biol.* **11**, 73 (1995); D. Hanahan and J. Folkman, *Cell* **86**, 353 (1996); J. Folkman, *Nature Biotechnol.* **15**, 510 (1997).
2. P. C. Brooks, R. A. F. Clark, D. A. Cheresh, *Science* **264**, 569 (1994); P. C. Brooks *et al.*, *Cell* **79**, 1157 (1994); M. Friedlander *et al.*, *Science* **270**, 1500 (1995); H. P. Hammes, M. Brownlee, A. Jonczyk, A. Sutter, K. T. Preissner, *Nature Med.* **2**, 529 (1996).
3. G. Martini-Baron and D. Marme, *Curr. Opin. Biotechnol.* **6**, 675 (1995); D. Hanahan, *Science* **277**, 48 (1997); W. Risau, *Nature* **386**, 671 (1997).
4. R. Pasqualini and E. Ruoslahti, *Nature* **380**, 364 (1996).
5. D. Rajotte *et al.*, in preparation.
6. Phage libraries were screened in mice carrying human MDA-MB-435 breast carcinoma xenografts as in (*4*, *10*). The structure of the libraries, the sequences recovered, and their prevalence (percent of insert sequenced) were as follows: $CX_3CX_3CX_3C$ library: CNGRCVSGCAGRC (26%), CGRECPRLCQSSC (15%), CGEACGGQCALPC (6%); CX_7C library: CDCRGDCFC (80%), CTCVSTLSC (5%), CFRDFLATC (5%), CSHLTRNRC (5%), CDAMLSARC (5%); CX_5C library: CGSLVRC (35%), CGLSDSC (12%), CYTADPC (8%), CDDSWKC (8%), CPRGSRC (4%).
7. E. Ruoslahti, *Annu. Rev. Cell Dev. Biol.* **12**, 697 (1996).
8. Abbreviations for the amino acid residues are as follows: A, Ala; C, Cys; D, Asp; E, Glu; F, Phe; G, Gly; H, His; I, Ile; K, Lys; L, Leu; M, Met; N, Asn; P, Pro; Q, Gln; R, Arg; S, Ser; T, Thr; V, Val; W, Trp; and Y, Tyr.
9. E. Koivunen, B. Wang, E. Ruoslahti, *Biotechnology* **13**, 265 (1995).
10. R. Pasqualini, E. Koivunen, E. Ruoslahti, *Nature Biotechnol.* **15**, 542 (1997).
11. E. Koivunen, D. Gay, E. Ruoslahti, *J. Biol. Chem.* **268**, 20205 (1993); E. Koivunen, B. Wang, E. Ruoslahti, *J. Cell Biol.* **124**, 373 (1994); J. M. Healy *et al.*, *Biochemistry* **34**, 3948 (1995).
12. W. Arap, R. Pasqualini, E. Ruoslahti, unpublished data.
13. Tumor-bearing mice (*10*) were anesthetized with Avertin intraperitoneally and phage or drugs were administered into the tail vein. All animal experimentation was reviewed and approved by the institute's Animal Research Committee.
14. R. K. Jain, *Cancer Metastasis Rev.* **9**, 253 (1996); C. H. Blood and B. R. Zetter, *Biochim. Biophys. Acta* **1032**, 89 (1990); H. F. Dvorak, J. A. Nagy, A. M. Dvorak, *Cancer Cells* **3**, 77 (1991); T. R. Shockley *et al.*, *Ann. N.Y. Acad. Sci.* **618**, 367 (1991).
15. M. S. Bretscher, *EMBO J.* **8**, 1341 (1989); S. L. Hart *et al.*, *J. Biol. Chem.* **269**, 12468 (1994).
16. A complete immunostaining panel of control organs is available online at www.burnham-inst.org/papers/arapetal.
17. M. R. Getter, M. E. Trigg, C. R. Merril, *Nature* **246**, 221 (1973).
18. The peptides RGD-4C (*9*, *10*), CNGRC, CGSLVRC, and GACVFSIAHECGA were synthesized, cyclized at high dilution, and purified by high-performance liquid chromatography (HPLC). The peptides were conjugated to dox (Aldrich) with 1-ethyl-3-(3-dimethyl-aminopropyl) carbodiimide hydrochloride (EDC; Sigma) and *N*-hydroxysuccinimide (NHS; Sigma) [S. Bauminger and M. Wilcheck, *Methods Enzymol.* **70**, 151 (1980)]. The conjugates were freed of reactants by gel filtration on a Sephadex G25 and contained <5% free drug, as assessed by HPLC and nuclear magnetic resonance (NMR). The carbodiimide conjugation method precluded a determination of the stoichiometry of the conjugates by mass spectrometry. Preliminary experiments (*12*) with a compound prepared by a different chemistry [A. Nagy *et al.*, *Proc. Natl. Acad. Sci. U.S.A.* **93**, 7269 (1996)] were homogeneous by HPLC, had a peptide-dox ratio of 1, and had an antitumor activity similar to that of the carbodiimide conjugates.
19. R. Steiner, in *Angiogenesis: Key Principles—Science, Technology and Medicine*, R. Steiner, P. B. Weisz, R. Langer, Eds. (Birkhauser, Basel, Switzerland, 1992), pp. 449–454.
20. D. P. Berger, B. R. Winterhalter, H. H. Fiebig, in *The Nude Mouse in Oncology Research*, E. Boven and B. Winograd, Eds. (CRC Press, Boca Raton, FL, 1991), pp. 165–184.
21. The concentration of dox was adjusted by measuring the absorbance of the drug and conjugates at 490 nm. A calibration curve for dox was used to calculate the dox-equivalent concentrations. Experiments with MDA-MB-435 cells and activated endothelial cells in vitro showed that the conjugation process did not affect the cytotoxicity of dox after conjugation.
22. M. Sakamoto, R. Pasqualini, E. Ruoslahti, unpublished data.
23. R. Max *et al.*, *Int. J. Cancer* **71**, 320 (1997); *ibid.* **72**, 706 (1997).
24. J. Denekamp, *Br. J. Radiol.* **66**, 181 (1993), F. J. Burrows and P. E. Thorpe, *Pharmacol. Ther.* **64**, 155 (1994); J. Folkman, in *Cancer: Principles and Practice of Oncology*, V. T. DeVita, S. Hellman, S. A. Rosenberg, Eds. (Lippincott, Philadelphia, 1997), pp. 3075–3085.

25. We thank E. Beutler, W. Fenical, and T. Friedmann for comments on the manuscript; N. Assa-Munt for NMR analysis; R. Kain, S. Krajewski, and M. Sakamoto for histological analysis; W. P. Tong for HPLC analysis; G. Alton and J. Etchinson for mass spectrometry analysis; E. Koivunen for a phage library; and S. Levinton-Kriss for the SLK cell line. Supported by grants CA74238-01, CA62042, and Cancer Center support grant CA30199 from the National Cancer Institute, and by the Susan G. Komen Breast Cancer Foundation.

9 September 1997; accepted 19 November 1997